Coupling effects in the elastic scattering of the exotic nucleus ^{6}He on protons

V. Lapoux, N. Alamanos, F. Auger, Y. Blumenfeld, J.M. Casandjian, M. Chartier, M.D. Cortina-Gil, V. Fekou-Youmbi, A. Gillibert, J.H. Kelley, et al.

Coupling effects in the elastic scattering of the exotic nucleus ^{6}He on protons

V. Lapoux [a], N. Alamanos [a], F. Auger [a], Y. Blumenfeld [b], J.-M. Casandjian [c], M. Chartier [c,1], M.D. Cortina-Gil [c,2], V. Fékou-Youmbi [a], A. Gillibert [a], J.H. Kelley [b,3], K.W. Kemper [d], M. Mac Cormick [b], F. Maréchal [b,4], F. Marie [a], W. Mittig [c], F. de Oliveira Santos [c], N.A. Orr [e], A. Ostrowski [c,5], S. Ottini-Hustache [a], P. Roussel-Chomaz [c], J.-A. Scarpaci [b], J.-L. Sida [a], T. Suomijärvi [b], J.S. Winfield [e,6]

[a] *CEA-SACLAY DSM/DAPNIA/SPhN F-91191, Gif-sur-Yvette, France*
[b] *IPN-Orsay, IN2P3-CNRS, 91406 Orsay Cedex, France*
[c] *GANIL, Bld Henri Becquerel, BP 5027, F-14021, Caen, France*
[d] *Physics Department, Florida State University, Tallahassee, FL 32306-4350, USA*
[e] *LPC-ISMRA, Bld du Maréchal Juin, F-14050, Caen, France*

Abstract

Cross sections for the elastic scattering of ^{6}He radioactive nuclear beam on proton targets have been measured at 38.3 MeV/nucleon. With a view to test the ability of general optical potentials to reproduce the data for scattering of unstable nuclei, the present results, as well as other existing data for ^{6,8}He, have been analyzed within the framework of the microscopic Jeukenne–Lejeune–Mahaux nucleon–nucleus potential. The angular distributions were found to be best reproduced by reducing the real part of the optical potential. This renormalization can be seen as a consequence of the complex polarization potential produced by the coupling to the continuum due to the weakly bound nature of the unstable nuclei. This effect can be simulated in a phenomenological analysis by a surface potential. © 2001 Published by Elsevier Science B.V.

PACS: 24.10.-i; 25.40.Cm; 25.60.-t; 27.20.+n

The weak binding of light neutron-rich nuclei leads to "exotic" features such as halos [1,2]. Nuclei such as ^{6}He exhibit much larger sizes than expected based on the short-range properties of the strong interaction. The halo is a direct consequence of the weak binding energies of the valence nucleons ($S_{2n}\{^6$He$\} = 975$ keV), which allows the wave functions to extend far from the core potential. The nucleus ^{6}He is the prototypical example of a two-neutron halo.

For reactions involving this nucleus, couplings to the continuum are expected to play a significant role since the scattering states are much closer to the continuum states than in stable nuclei. As such the standard description in terms of well separated bound states from continuum states is no longer valid. In pioneering work describing the microscopic folding analysis of nucleus–nucleus elastic scattering [3], Satchler and Love proved that it was necessary to reduce the real part of the optical potential to reproduce the data involving light, weakly bound nuclei, such as ^{6}Li and ^{9}Be [3]. This renormalization was attributed directly to the coupling to the continuum states, favoured by the weak binding energy of these nuclei [4]. These effects are not taken into account in approaches employing optical potentials [5].

Nucleus–nucleon elastic scattering can be described using the complex microscopic JLM potential [6] which only depends on the scattering energy and on the neutron and proton densities of the nucleus. The potential is deduced from calculations in infinite symmetric nuclear matter with the Brueckner matrix including the Reid hard-core nucleon–nucleon interaction. For nucleon energies up to 160 MeV, the nucleus–nucleon potential is obtained by applying the local density approximation. In the case of stable nuclei, this approach reproduces successfully a large range of proton and neutron elastic scattering angular distributions [7]. For light nuclei, it was demonstrated [8] that the JLM potential could reproduce the data by renormalizing the imaginary potential ($\lambda_W \sim 0.8$) and without any renormalization of the real part ($\lambda_V = 1$). This prescription will be referred to below as the "standard JLM".

As an example of the validity of the JLM potential for the light nuclei we present in the Fig. 1 our analysis for the elastic scattering of ^{7}Li(p, p) measured at 24.4 MeV [9] and of p(^{7}Li, ^{7}Li) at 65 MeV [10]. The JLM potential is calculated with a simple Gaussian
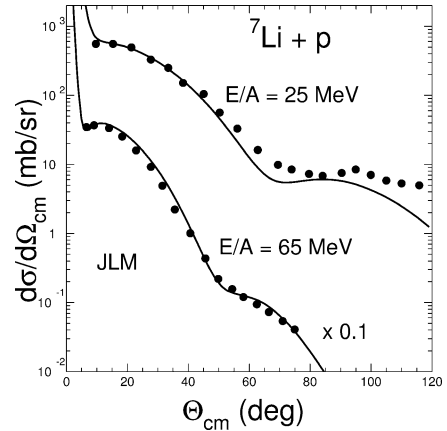

Fig. 1. Cross sections for the ^{7}Li + p elastic scattering compared to calculations using the JLM potential. Data are from Ref. [9,10].

form for the ^{7}Li proton and neutron densities. Their root mean square (rms) radii are 2.279 and 2.441 fm, respectively, as given in Ref. [3]. The data at the two energies are well reproduced by the standard JLM potential. A set of elastic data of light nuclei on protons was presented in a previous article [11], including ^{6}He. The microscopic JLM optical potential was used to perform the calculations of the elastic potential. For comparison, the CH89 parametrization [12] was also used. CH89 is a phenomenological optical potential which uses standard form factors for the potential, with the depth and geometry determined by fitting a large amount of differential cross sections for proton and neutron elastic scattering on nuclei with mass numbers ranging from 40 to 209 and in the energy domain of 10–65 MeV. The data were well reproduced using both potentials provided that the real part was reduced or the imaginary part enhanced. This was attributed to the couplings necessary for the weakly bound nuclei. Importantly, however, the two renormalizations (real or imaginary) led to very different cross sections at large angles. Unfortunately, the data did not extend to large enough angles to allow the correct renormalization to be identified.

It is then necessary to extend to large angles the previous measurements that were limited to 40° c.m. (center of mass) for ^{6}He.

In this spirit we have remeasured cross sections for elastic hydrogen (polypropylene) target. The differential cross sections were measured from 1.35° to 8.55° in the laboratory. The c.m. angle range covered was

from 9.5° to 71.5°. It has thus proven possible to investigate more comprehensively the effect of the weak binding on the elastic scattering and to test the validity of the general nucleus–nucleon optical potentials. The experiment was undertaken at the GANIL coupled cyclotron facility. The ^{6}He secondary beam was produced by fragmentation of a 75 MeV/nucleon primary ^{13}C beam on a carbon production target located between the two superconducting solenoids of the SISSI device [13]. The secondary beam was purified with an achromatic degrader set in the beam analysis spectrometer [14]. The ^{6}He beam was produced at an energy of 38.3 MeV/nucleon and an intensity of 10^5 pps (particles per second). Elastic angular-dependent cross sections of ^{6}He projectiles that were scattered from a 10 mg/cm^2 thick polypropylene target (CH$_2$ CHCH$_3$)$_n$ (density 0.896 g/cm^3) were measured with the SPEG dispersion-matched energy-loss spectrometer [15]. The scattered particles were identified at the focal plane by the energy loss measured in an ionisation chamber and the residual energy measured in a thick plastic scintillator. The momentum and the angle after the target were obtained by track reconstruction of the trajectories as determined by two drift chambers straddling the focal plane of the spectrometer. The position and incident angle of the projectiles on the target were determined event-by-event using two position sensitive detectors located upstream of the target. The scattering angle was then calculated by taking into account the incident angle.

The polypropylene target contains both hydrogen and carbon nuclei allowing a simultaneous measurement of the cross sections on ^{12}C and protons. Owing to the good energy resolution of the SPEG spectrometer ($\Delta E/E = 10^{-3}$), the elastic scattering data did not include contamination from scattering to the ^{12}C excited states. Cross sections on ^{12}C are dominated at small angles by Coulomb deflection, so the calculation at these angles is not sensitive to the nuclear potential. Consequently, all calculations lead to the same first maximum of the angular distribution, thus providing an absolute normalization for the data on ^{12}C, and as a result on the protons. The normalization error which results from the uncertainties due to the target thickness, the number of incident particles and the acceptance of the detection system is thus negligible compared to the statistical one. The data for the elastic scattering of ^{6}He on protons are presented in Fig. 2. In
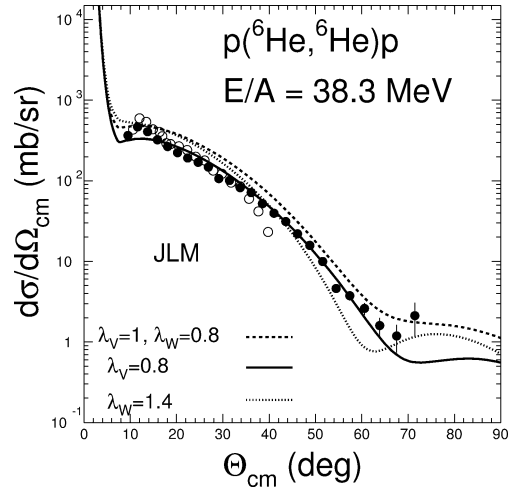

Fig. 2. Cross sections for the ^{6}He + p elastic scattering at 38.3 MeV/nucleon compared to calculations using the JLM potential. The full circles correspond to the present data. The open circles are the data measured at 41.6 MeV/nucleon in a previous experiment [11].

the figure, the uncertainties are statistical. The binning of the data presented in Fig. 2 corresponds to the angular resolution of the measurement, which is equal to 0.3° in the laboratory system. In the c.m. frame, the spacing between points is of the order of 2.1° at the smaller angles (from 9.5°–11.6°) and increases to 4° c.m. for the final angles (67.4°–71.5°) due to the kinematics. First, the elastic scattering is calculated with the JLM potential. In a three-body model [16], ^{6}He can be described as a tightly bound alpha particle plus two valence neutrons. The ^{6}He density used in the JLM calculation was a three-body density with a matter rms radius of 2.55 fm, which is close to the value obtained in the three-body model analysis [17] of the elastic scattering of ^{6}He by protons at 700 MeV/nucleon [18]. All theoretical curves are folded with the experimental angular resolution. In the angular range from 15° to 50° c.m., there is a large discrepancy between the standard JLM curve ($\lambda_v = 1$ and $\lambda_W = 0.8$) and the data.

To improve the agreement with the data, we tried two approaches. First we normalized the real part of the nuclear potential by a factor $\lambda_v = 0.8$ ($\lambda_W = 0.8$); then we normalized the imaginary part by $\lambda_W = 1.4$ (keeping $\lambda_v = 1.0$). The JLM analysis is presented in Fig. 2.
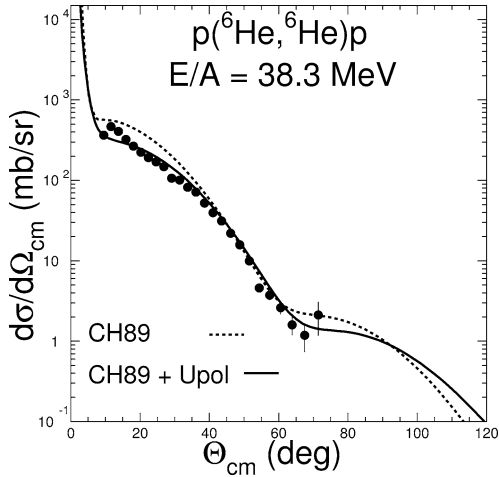
Fig. 3. Cross sections for the ^{6}He + p elastic scattering compared with calculations using the CH89 potential (dashed line) and taking into account a complex polarization potential (solid line). The parameters of the DPP are given in the text.

The angular distributions of ^{6}He on protons are better reproduced when the real part of the JLM potential is reduced (Fig. 2), with a factor 0.8. The origin of this effect was discussed in Ref. [5] and may be explained within the theory developed by Feshbach [19]. According to this theory, the interaction potential should be written as $U = V + U_{pol}$ where V is the usual real potential and U_{pol} is the dynamical polarization potential (DPP). V can be seen as the folding potential or the elastic potential described by microscopic or phenomenological models. It includes only the interaction between the projectile and the target ground states. U_{pol} is complex, non-local and energy-dependent, it arises from couplings to inelastic channels. With $U_{pol} = V_{pol} + i W_{pol}$, the total optical potential can be written as $U = V + V_{pol} + i W$ with W including W_{pol}. For well-bound nuclei, the excitation probability during the elastic scattering is weak, and the main contribution is imaginary, represented by the usual phenomenological imaginary part W which is added to the real V to form the optical potential. For weakly-bound nuclei, the enhancement of the coupling to the continuum leads to a greater influence of U_{pol} and then to the reduction of the real part of the nuclear potential. This corresponds to the effect observed in ^{6}He + p scattering, as analyzed using the JLM potential (Fig. 2).

We now want to obtain a simple expression of the DPP for the elastic ^{6}He + p potential. A complex surface potential, with a repulsive real part, is expected to simulate the surface effects generated by the polarization potential [4]. Microscopic features of the DPP were obtained in Ref. [20] in the case of the system ^{11}Li + ^{12}C, and this study indicated the general behavior of the DPP, that was used in Ref. [21] to represent the DPP in a very simple way. As in Ref. [21], we have adopted a potential of Woods–Saxon first derivative shape, with radius parameter $R_0 = 0$:

$$U_{pol} = -\frac{(V_{pol} + i W_{pol}) \exp(r/a_{pol})}{[1 + \exp(r/a_{pol})]^2}.$$

Its parameters V_{pol}, W_{pol} and a_{pol} are adjusted on the data. Since the effect of the coupling corresponds to the reduction of the total interaction potential, the resulting DPP is expected to be repulsive. The DPP written above has a very simple shape and no microscopic inputs. The objective here is only to show that a phenomenological DPP, added to the elastic potential, can account for the effects of the couplings induced by the weak binding energy of the nucleus ^{6}He. Then, in the following analysis, instead of the JLM potential used before, we have adopted for simplicity the CH89 optical potential parametrization [12] and the DPP U_{pol} described above is added to the CH89 potential for the ^{6}He + p reaction at 38.3 MeV/nucleon [22]. This will provide the complete parametrization of the ^{6}He + p potential, useful to predict cross sections. Moreover, this parametrized potential can be compared easily with potentials given for other weakly bound systems. With the sign conventions of CH89 (its real part is written $-V/(1 + \exp[(r - R)/a])$ with $V > 0$) the parameters of the DPP are $V_{pol} = -47.2$ MeV, $W_{pol} = -4.4$ MeV and $a_{pol} = 1.33$ fm. Since the sign of $\Re e\, U_{pol}$ and $\Im m\, U_{pol}$ is positive, the DPP added to CH89 reduces the interaction potential. The elastic cross sections are then calculated with the ECIS97 code [23]. The result for the ^{6}He + p system is given in Fig. 3. As for the JLM, the CH89 potential alone does not allow the data below 40° (dashed line) to be reproduced. But if we take into account the effects generated by the polarization potential, and use the DPP, the ^{6}He + p data are well reproduced (solid line). A similar analysis, using the repulsive DPP, could be done with the JLM potential, instead of the CH89 potential.
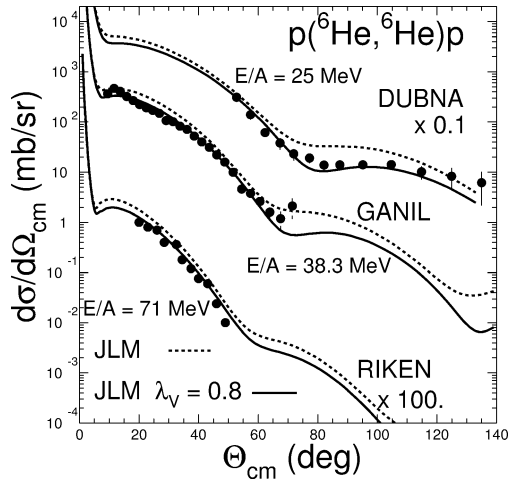
Fig. 4. The present ^{6}He + p data (GANIL) together with data obtained at Dubna [25] and at Riken [26]. The lines are the results of calculations using the JLM potential.

Fig. 5. Cross sections for the ^{8}He + p elastic scattering. The lines are the results of calculations using the JLM potential.

Both the phenomenological DPP and the normalization procedure applied to the JLM potential for ^{6}He + p at 38.3 MeV/nucleon have reproduced the data. The DPP was studied in Ref. [24] for the elastic scattering of the weakly bound ^{11}Li on ^{12}C at 60 MeV/nucleon, and it was shown that the two approaches were not equivalent to describe the scattering refractive patterns at larger angles. Here, for the elastic scattering on protons, both methods provide a global description of the decrease in differential cross sections related to the coupling to the continuum, and for an angular range up to 70°. To confirm our findings, we have reanalyzed other proton elastic scattering data for ^{6}He projectiles that were measured at Dubna [25] and Riken [26]. As seen in Fig. 4, the renormalization by a factor of 0.8 (solid line) of the real part of the JLM potential also allows the sets of data for ^{6}He, obtained at 25 and 71 MeV/nucleon, to be reproduced.

We now consider the nucleus ^{8}He and the data taken at Riken [26]. Here we are dealing with a weakly bound nucleus ($S_{4n} = 3.1$ MeV), with no bound excited states and low-lying resonances [27,28]. As done for the ^{6}He + p scattering, it is possible to reproduce these ^{8}He + p data using a phenomenological DPP [29], with the same shape as presented previously. Within the five-body COSMA model [28], ^{8}He is described as an inert alpha core with four valence neutrons occupying a full $0p_{3/2}$ subshell and constitut-
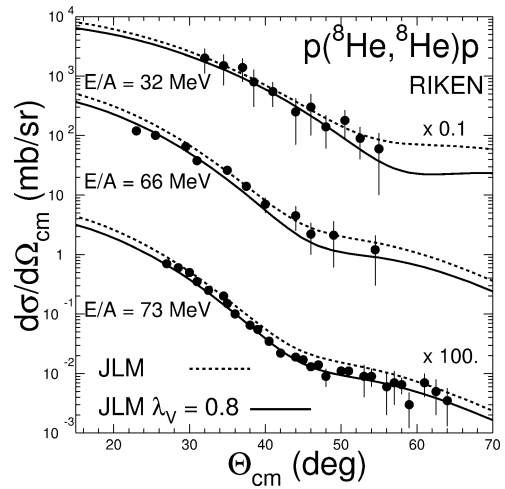
ing a neutron skin. With the same normalization procedure of the JLM potential adopted in the case of ^{6}He, elastic scattering of ^{8}He on protons [26] at 32, at 66 and at 73 MeV/nucleon has been analyzed using the COSMA densities [28] that yield an ^{8}He matter rms radius of 2.52 fm. The calculations reproduce successfully the data (Fig. 5) at 73 MeV/nucleon, provided that the real part of the potential is renormalized by 0.8. At 32 and 66 MeV/nucleon, the statistical quality of the data is quite low and we can only conclude that data are consistent with such a renormalization.

Recently, a description of the elastic scattering of ^{9}Be (its threshold to one neutron emission is very low $S_n = 1.67$ MeV) was successfully undertaken with the reduction of the elastic potential by a factor of $\sim 40\%$ [30]. Such a reduction may also influence inelastic scattering and fusion reactions, and may explain why the data for fusion in the system ^{9}Be + ^{209}Pb reported in Ref. [31] are overestimated by the calculations. This phenomenon was underlined in Ref. [3] and theoretically demonstrated in Ref. [4] for the elastic scattering of stable weakly bound nuclei: it was shown that coupling to the continuum for ^{6}Li produces a surface reduction of the usual elastic potential.

As a consequence of the causality principle, a dispersion relation links the energy dependencies of the real and the imaginary parts of the optical potential, as explained in Ref. [32]. Through these relations, the dispersive contribution which arises from the coupling

between the elastic and non-elastic channels can be evaluated, as done in Ref. [33]. It can be expected that these dispersion relations should constrain the DPP. Nevertheless, it was shown that the weakly bound systems may not display the same features, concerning these relations, as the stable nuclei do. It has been established for many systems of stable nuclei that the energy dependence of the elastic potential around the Coulomb barrier is described by the dispersion relations and corresponds to the so-called threshold anomaly [34,35]: a localized peak in the strength of the real part V, around the Coulomb barrier, associated to a sharp increase with energy near the threshold in the imaginary part W. But in the case of weakly bound nuclei, the absence of the anomaly was theoretically discussed by Mahaux, Ngô and Satchler [32]: couplings between break-up and elastic channels gives rise to a large repulsive real polarization potential and to a weak imaginary potential, that is almost energy independent. Recently, potentials have been deduced from the elastic scattering data involving the weakly bound nucleus ^{6}Li, and the absence of the anomaly was shown [36,37]. Therefore, since the loosely bound systems may not display a threshold anomaly, we cannot base upon the dispersion relations to get the correct behavior for the DPP. Elastic scattering data are needed to deduce the interaction potential at the right energy.

In summary, we have measured elastic scattering by protons of the radioactive neutron-rich nucleus ^{6}He. The interaction potential between the nucleus and protons was calculated within the framework of the JLM optical potential. It was demonstrated that a normalization factor on the real potential was needed to reproduce the data. This suggests that the coupling of the ground state to possible low lying resonant states in the continuum predominantly affects the real part of the potential. A complex surface potential, with a repulsive real part, was added to the CH89 optical potential to simulate the surface effects generated by the polarization potential. The features deduced for the polarization potential are in agreement with the theoretical work made by Y. Sakuragi [4]. Here, we have shown that it is a more general effect, and proven that the weak binding of nuclei far from the valley of stability results in an increase of the couplings to the continuum, which in turn leads to an enhancement of the polarization potential and then to the decrease of

the real part of the elastic potential. Our data would require a precise treatment of the polarization potential through an explicit calculation of the coupling, as done with the continuum discretized coupled channel methods [4]. But this involves the knowledge of the couplings to low-lying resonant states of the system for which additional data are needed. These effects must be taken into account in the study of reaction mechanisms at low energy.

Acknowledgements

References

[1] P.G. Hansen, B. Jonson, Europhys. Lett. 4 (1987) 409.
[2] S.N. Ershov et al., Phys. Rev. C 56 (1997) 1483.
[3] G.R. Satchler, W.G. Love, Phys. Rep. 55 (1979) 183.
[4] Y. Sakuragi, Phys. Rev. C 35 (1987) 2161.
[5] M.E. Brandan, G.R. Satchler, Phys. Rep. 285 (1997) 143.
[6] J.P. Jeukenne, A. Lejeune, C. Mahaux, Phys. Rev. C 16 (1977) 80, and references therein.
[7] S. Mellema, R. Finlay, F. Dietrich, F. Petrovich, Phys. Rev. C 28 (1983) 2267.
[8] J.S. Petler et al., Phys. Rev. C 32 (1985) 673.
[9] F. Petrovich et al., Nucl. Phys. A 563 (1993) 387.
[10] C.B. Moon et al., Phys. Lett. B 297 (1992) 39, and references therein.
[11] M.D. Cortina-Gil et al., Phys. Lett. B 401 (1997) 9.
[12] R.L. Varner et al., Phys. Rep. 201 (1991) 57.
[13] A. Joubert et al., in: Particle Accelerator Conference, Vol. 1, IEEE, 1991, p. 594.
[14] R. Anne et al., Nucl. Instrum. Methods Phys. Res. A 257 (1987) 215.
[15] L. Bianchi et al., Nucl. Instrum. Methods Phys. Res. A 276 (1989) 509.
[16] B.V. Danilin, M.V. Zhukov, J.S. Vaagen, J.M. Bang, Phys. Lett. B 302 (1993) 129.
[17] J.S. Al-Khalili, J.A. Tostevin, I.J. Thompson, Phys. Rev. C 54 (1996) 1843.
[18] G.D. Alkhazov et al., Phys. Rev. Lett. 78 (1997) 2313.
[19] H. Feshbach, Ann. Phys. 5 (1958) 357.
[20] K. Yabana, Y. Ogawa, Y. Suzuki, Phys. Rev. C 45 (1992) 2909.
[21] M. Hussein, G.R. Satchler, Nucl. Phys. A 567 (1994) 165.
[22] V. Lapoux et al., in: Proceedings of International Symposium on Quasiparticle and Phonon Excitations in Nuclei, RIKEN, Japan, December 4–7, 1999, World Scientific, Singapore, 2000.

[23] J. Raynal, Phys. Rev. C 23 (1981) 2571;
J. Raynal, ECIS97, private communication.

[24] D.T. Khoa, G.R. Satchler, W. von Oertzen, Phys. Lett. B 358 (1995) 14.

[25] R. Wolski et al., Phys. Lett. B 467 (1999) 8.

[26] A.A. Korsheninnikov et al., Nucl. Phys. A 617 (1997) 45.

[27] A.A. Korsheninnikov et al., Phys. Lett. B 316 (1993) 38.

[28] M.V. Zhukov, A.A. Korsheninnikov, M.H. Smelberg, Phys. Rev. C 50 (1994) R1.

[29] V. Lapoux, PhD Thesis, Université d'Orsay, 1998, DAPNIA/SPHN-98-05T.

[30] L. Trache et al., Phys. Rev. C 61 (2000) 02461.

[31] M. Dasgupta et al., Phys. Lett. B 82 (1999) 1395.

[32] C. Mahaux, H. Ngô, G.R. Satchler, Nucl. Phys. A 449 (1986) 354.

[33] C. Mahaux, R. Sartor, Nucl. Phys. A 460 (1986) 466.

[34] M.A. Nagarajan, G.R. Satchler, Phys. Lett. B 173 (1986) 29.

[35] G.R. Satchler et al., Ann. Phys. 178 (1987) 110.

[36] M.A. Tiede, D.E. Trcka, K.W. Kemper, Phys. Rev. C 44 (1991) 1698.

[37] N. Keeley et al., Nucl. Phys. A 571 (1994) 326;
N. Keeley, K. Rusek, Phys. Lett. B 427 (1998) 1.